Biomaterials 34 (2013) 1987–1994

Contents lists available at SciVerse ScienceDirect

Biomaterials

journal homepage: www.elsevier.com/locate/biomaterials

Superparamagnetic iron oxide nanoparticle targeting of MSCs in vascular injury

Johannes Riegler [a,b,*], Aaron Liew [c], Sean O. Hynes [c], Daniel Ortega [d], Timothy O'Brien [c], Richard M. Day [e], Toby Richards [f], Faisal Sharif [c], Quentin A. Pankhurst [d,g], Mark F. Lythgoe [a]

[a] Centre for Advanced Biomedical Imaging (CABI), Department of Medicine and Institute of Child Health, University College London (UCL), London WC1E 6DD, UK
[b] Centre for Mathematics and Physics in the Life Sciences and Experimental Biology (CoMPLEX), UCL, London WC1E 6BT, UK
[c] Regenerative Medicine Institute (REMEDI), National Centre for Biomedical Engineering and Science (NCBES), National University of Ireland, Galway, Ireland
[d] Davy-Faraday Research Laboratory, The Royal Institution of Great Britain, London W1S 4BS, UK
[e] Centre for Gastroenterology & Nutrition, Division of Medicine, University College London, WC1E 6DD, UK
[f] Division of Surgery and Interventional Science, University College Hospital, London WC1E 6AU, UK
[g] Institute of Biomedical Engineering, University College London, Gower Street, London WC1E 6BT, UK

ARTICLE INFO

Article history:
Received 2 October 2012
Accepted 22 November 2012
Available online 11 December 2012

Keywords:
Magnetic targeting
Stem cell
Nanoparticle
Restenosis
Catheter

ABSTRACT

Vascular occlusion can result in fatal myocardial infarction, stroke or loss of limb in peripheral arterial disease. Interventional balloon angioplasty is a common first line procedure for vascular disease treatment, but long term success is limited by restenosis and neointimal hyperplasia. Cellular therapies have been proposed to mitigate these issues; however efficacy is low, in part due to poor cell retention. We show that magnetic targeting of mesenchymal stem cells gives rise to a 6-fold increase in cell retention following balloon angioplasty in a rabbit model using a clinically applicable permanent magnet. Cells labelled with superparamagnetic iron oxide nanoparticles exhibit no negative effects on cell viability, differentiation or secretion patterns. The increase in stem cell retention leads to a reduction in restenosis three weeks after cell delivery.

1. Introduction

Cardiovascular disease remains the most common cause of death in industrialised countries despite continuous progress in detection and treatment. A major cause for these diseases is atherosclerosis which leads to arterial occlusion causing nutrient and oxygen deprivation [1,2]. First line treatment of cardiovascular and peripheral arterial disease frequently includes balloon angioplasty, with or without the deployment of stents [3–6]. Procedure associated injuries to the vessel wall such as barotrauma and denudation induce a vascular response that can lead to the restenosis and occlusion of the treated artery [7–9]. The introduction of stents and in particular drug eluting stents has reduced the rate of restenosis, but it remains a significant problem [10].

Cellular therapies are an attractive option as adjunct therapies, improving endothelial repair and preventing restenosis [11–13]. Maximising cell retention and limiting the risk of unwanted side effects demands an efficient delivery technique. Magnetic targeting is ideally suited to augment cellular therapies by guiding cells to sites of injury using externally generated magnetic fields and field gradients [14]. Previous studies have shown the feasibility of magnetic cell targeting [15–17]. However, most of these studies have used strong magnets placed directly next to the artery, limiting their potential for clinical translation [16–18]. Inevitably the short distance between magnet and target artery ensures strong magnetic forces leading to favourable outcomes. Unfortunately such high forces cannot be achieved for human dimensions as magnetic forces decline rapidly with increased distance between magnet and artery. To address this issue of scalability, we have previously performed theoretical optimisations to design a magnet for magnetic cell delivery to human lower leg arteries which generates uniform forces along the peroneal, anterior and posterior tibial arteries [19]. Based on these results, we have designed and built a scaled-down appliance suitable for experiments with rabbits, which can readily be translated into a clinical device. We have used this in a balloon catheter intervention in which blood flow cessation was limited to less than 5 min as in the clinical setting.

Cellular therapies for the treatment of arterial injury have explored the use of bone marrow cells [20,21], endothelial

* Corresponding author. Stanford University, School of Medicine, 259 Campus Drive, Grant Building S111, Stanford, CA 94305, USA. Tel.: +1 650 387 4685; fax: +1 650 723 6272.
E-mail address: j.riegler@stanford.edu (J. Riegler).

0142-9612/$ – see front matter © 2012 Elsevier Ltd. All rights reserved.
http://dx.doi.org/10.1016/j.biomaterials.2012.11.040

progenitor cells (EPCs) [11–13,22] and mesenchymal stem cells (MSCs) [23,24]. Several studies have demonstrated the reduction of restenosis after EPC delivery although primarily with initial cessation of blood flow for 20 min to increase cell attachment [11–13]. Delivered EPCs were found to speed up re-endothelisation via integration into the new endothelial layer [11,12]. A limited number of studies have assessed the effect of MSC delivery on endothelisation and restenosis, while no data is available for the effect of magnetic MSC delivery in this context. We have therefore developed a new magnetic targeting device that has enhanced cell retention and subsequently reduced restenosis following interventional angioplasty, which can readily be applied to vascular injury in the clinical setting.

2. Materials and methods

2.1. Superparamagnetic iron oxide nanoparticles (SPIONs)

Commercially available nanoparticles FluidMAG-D, FluidMAG-lipid, FluidMAG-DEAE, FluidMAG-P, FluidMAG-Q (Chemicell GmbH), Endorem (Guerbet S.A.) and Ferucarbotran (Meito Sangyo Co Ltd.) were used for this study. Particle characteristics were measured using a Zetasizer Nano ZS (Malvern Ltd.) and a super conduction quantum interference device (SQUID) (Quantum Design Inc) (see Supplementary information for details).

2.2. MSC labelling

Rabbit mesenchymal stem cells (MSCs) were established and cultured in MSC medium. MSCs were plated in 96 well plates (10,000 cells/well) and incubated for 24 h with increasing concentrations of SPIONs with or without 2 h of serum starvation (serum starvation can lead to increased particle internalisation) prior to particle addition. Following that, cells were washed twice and the metabolic activity of cells was measured using an MTS assay following manufactures instructions (Invitrogen Ltd.). SPION concentrations which preserved at least 95% viability (metabolic activity) were used to label MSCs for SQUID measurements, Prussian blue staining and transmission electron microscopy (see Supplementary information for details). MSC labelling for 24 h with 0.62 mg FluidMAG-D per ml media was used for the rest of the *in vitro* and *in vivo* experiments.

2.3. MSC differentiation and secretion profile

MSCs labelled with FluidMAG-D and unlabelled control cells were differentiated following standard protocols. Secretion levels of growth factors and cytokines of labelled and unlabelled cells were assessed with an angiogenesis array following the manufacturer's instructions (R&D Systems Inc.) (see Supplementary information for details).

2.4. Magnetic resonance imaging of cell and artery samples

All MRI experiments were performed on a horizontal bore 9.4 T DirectDrive VNMRS system (Agilent Technologies Inc.). Increasing concentrations of labelled cells ($3\bullet10^4$ to $1\bullet10^6$) in 1% agar were filled into tubes and used for T_2 and T_2^*

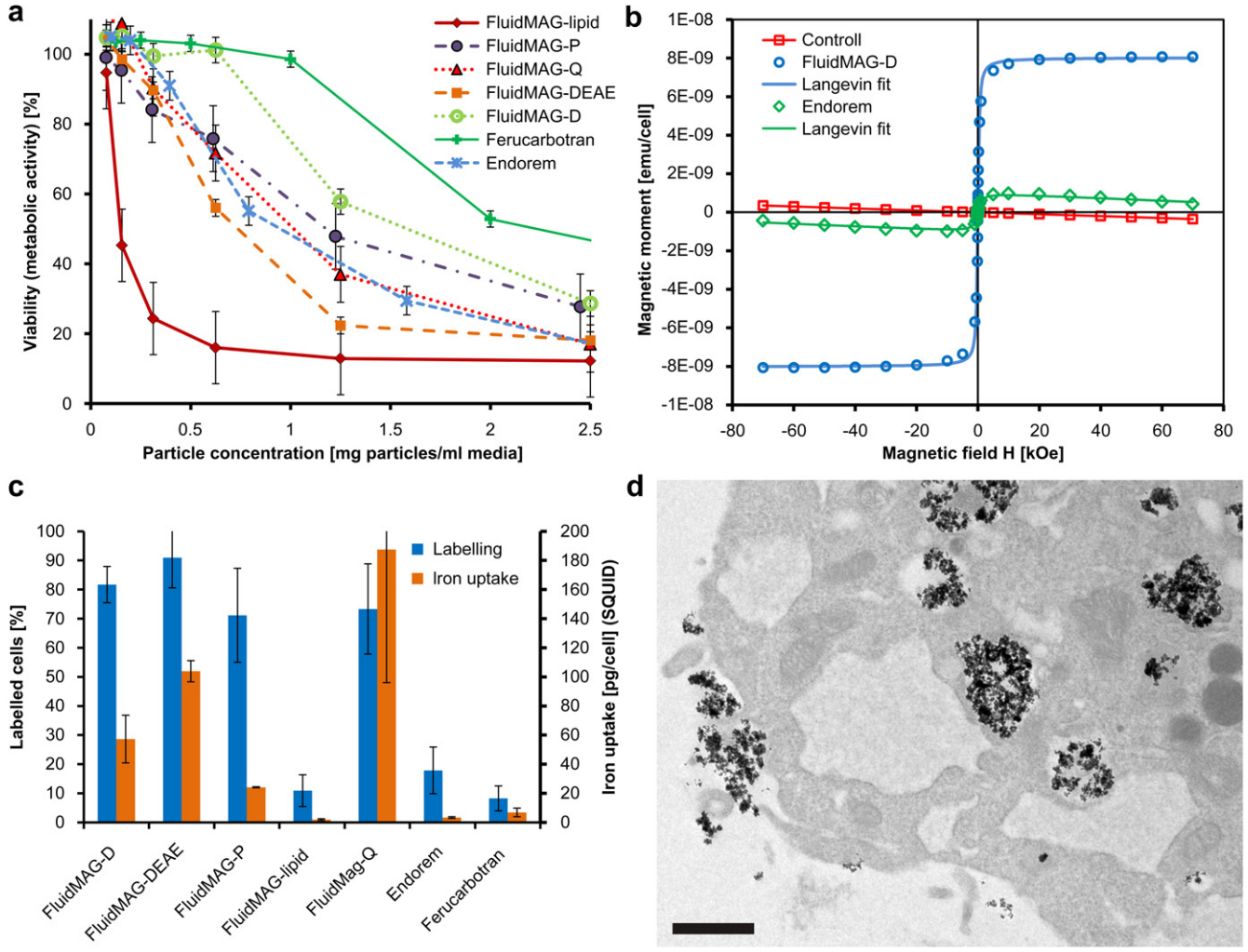

Fig. 1. Metabolic activity (a) of cells labelled with different concentrations of iron oxide nanoparticle formulations seeded together with cells. Magnetisation versus magnetic field (M–H) plots (b) for unlabelled control cells (red), weakly labelled cells (Endorem, green) and strongly labelled cells (FluidMAG-D, blue). SQUID measurements of iron oxide nanoparticle internalisation (c) (orange bars) for different iron oxide based particles as well as percentage of labelled cells (blue bars). Transmission electron microscope image (d) of particle distribution in a cell labelled with fluidMAG-D (0.65 mg nanoparticles/ml culture media) (scale bar: 1 μm). (For interpretation of the references to colour in this figure legend, the reader is referred to the web version of this article.)

measurements. Artery samples ($n = 4$) were harvested 24 h after cell delivery, flashed with saline and fixed overnight in formalin. Fixed arteries were suspended in PBS containing 8 mM Gadolinium (Magnevist, Bayer AG) for high resolution (40 μm isotropic) 3D gradient echo imaging (see Supplementary information for details).

2.5. Cell attachment and label dilution

Magnetically and fluorescently (PKH26, Sigma) labelled MSCs or unlabelled control cells were seeded into 6-well plates (30,000 per well) and incubated with or without the presence of a magnetic field. Bottom surfaces of these 6 well plates were covered with a HUVEC monolayer or coated with fibronectin. Cell suspensions were removed after 15, 30, 45, 60, 90 and 120 min of incubation, wells were washed with PBS, filled with fresh media and images were acquired with a light microscope (Axiovert, Carl Zeiss AG). Automatic cell counting was used to estimate the number of cells attached to the surface.

To estimate iron oxide nanoparticle dilution due to cell growth, magnetically labelled MSCs were cultured for two weeks while samples were taken after each passage (500,000 cells) and used for SQUID measurements (see Supplementary information for details).

2.6. Rabbit arterial injury model for in vivo cell delivery

Animal experiments were performed in accordance with national regulations set forth by the Department of Health and Children, Ireland (Lic. Nr. B100/3518) and were approved by the institutional animal care committee. A total of 16 male New Zealand White rabbits (Harlan, Bicester, UK) weighing 2.0–2.5 kg were used. Animals were fed a standard chow diet and water ad libitum. Rabbits received daily oral Aspirin starting one week prior to surgical procedures.

In vivo balloon injury and cell delivery model: A 5-French introducer sheath (Radifocus, Terumo, NJ, USA) was surgically introduced into the right carotid artery and advanced to the lower abdominal aorta. A balloon injury was performed with a 2.0 × 15 mm balloon in the femoral artery (1 min, 12 atm) as described previously [25]. Following the initial injury, the balloon was deflated, moved 2 cm proximal to the injury position and inflated to a lower pressure suitable to stop blood flow. The guide wire was removed and 100,000 labelled MSCs in 300 μl saline were infused through the central lumen of the over the wire balloon within 1 min. Blood flow was restored 4 min thereafter and the balloon was retrieved. The same procedure was repeated on the contralateral femoral artery but an external cylindrical magnet (Halbach cylinder, Magnet Sales Ltd.) was placed around the respective leg after initial injury. Blood flow was restored 4 min after cell delivery; however, the external magnet was kept in place for an additional 40 min. Balloon and introducer were removed after cell delivery and the neck incision closed. Rabbits were closely monitored and kept anesthetized for the remaining magnet placement time. Rabbits were allowed to recover after anaesthesia in a warm comfortable environment (see Supplementary information for details).

2.7. Cell retention 24 h after delivery

Rabbits were sacrificed 24 h after cell delivery, right and left femoral arteries were extracted, flushed with saline, cut open longitudinally and fixed in a flattened position over night at 4 °C in 4% Formalin. Fixed samples were mounted in DAPI containing mounting media (Vectashield) for enface confocal microscopy (PerkinElmer Inc.). Fluorescently labelled cells were counted manually in a blinded fashion (see Supplementary information for details).

2.8. Restenosis and re-endothelialisation three weeks after MSC delivery

Rabbits were sacrificed 3 weeks after cell delivery, right and left femoral arteries were extracted, flushed with saline, fixed overnight in 4% Formalin and embedded in paraffin. Paraffin sections were stained with H&E for manual intima and media thickness measurements. Additional sections were stained with a CD31 antibody (ab9498, Abcam Ltd.) and the length of unstained versus total arterial lumen boundary was measured to estimate the degree of re-endothelialisation in a blinded fashion (see Supplementary information for details).

2.9. Statistical analysis

Experimental data were presented as means ± standard deviation. Results were evaluated using a Wilcoxon signed rank test or one way ANOVA where appropriate.

3. Results

3.1. MSC labelling with superparamagnetic iron oxide nanoparticles

To maximise the available magnetic force and maintain cellular functionality, internalisation of a range of commercially available

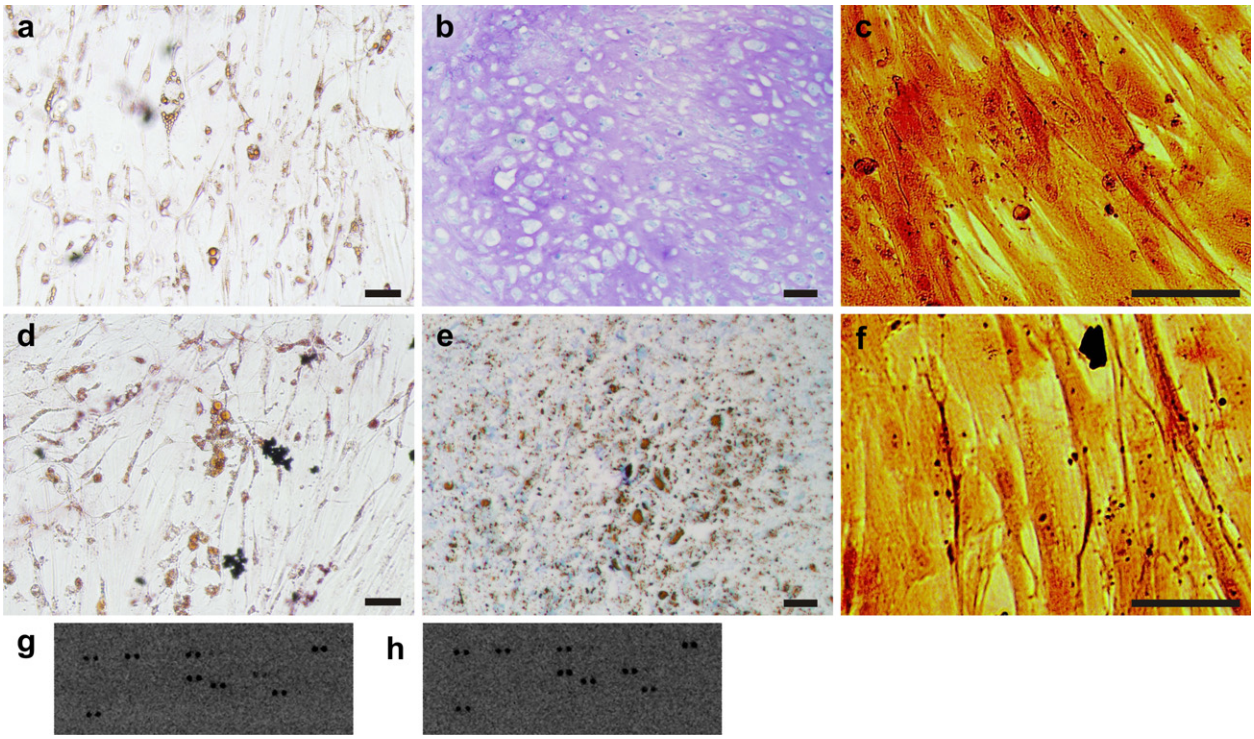

Fig. 2. Adipogenic (a), chondrogenic (b) and osteogenic (c) differentiation of unlabelled MSCs compared to magnetically labelled MCSs (d-f). The similar staining for fat globules (Oil red; a,d) and calcium repositioning (Stanbio Calcium; **c,**f) indicates that nanoparticle labelling had no effect on adipogenic and osteogenic differentiation respectively. However, chondrogenic differentiation was impaired as indicated by the difference in glycosaminoglycan staining (Toluidine blue; b,e). Secretion of proteins and growth factors for control (g) and magnetically labelled (h) MSCs was similar as indicated by binding of soluble factors to their respective spots on the angiogenesis array. (scale bar: 100 μm). (For interpretation of the references to colour in this figure legend, the reader is referred to the web version of this article.)

particles including MRI contrast agents was investigated (Supplementary Tab. S1). Cell viability varied with particle concentration and type (Fig. 1a). We selected particle concentrations which preserved at least 95% cell viability for further experiments. To test for a potential uptake improvement, we used serum starvation and noted increased particle uptake, except for FluidMAG-D, -DEAE and −Q, and a reduction in toxicity for FluidMAG-lipid (Supplementary Fig. S1-2). Investigating the degree of cellular internalisation of selected particles using SQUID magnetometry, we found high magnetic moments for FluidMAG-D, -DEAE, -P and −Q labelled cells (Fig. 1b,c). However, microscopic images showed that even after five washing steps, a significant amount of particles remained on the surface of MSCs when labelled with particles carrying a high positive charge, ruling out the further use of FluidMAG-DEAE and -Q (ζ-potential > 50 mV) (Supplementary Fig. S3, Tab. S1). Investigating cells with transmission electron microscopy (TEM) confirmed a marked internalisation of particles for FluidMAG-D and −P while low internalisation and high cell surface accumulation were found for FluidMAG-DEAE and-Q (Fig. 1d, Supplementary Fig. S4). Particles were observed in endosome-like structures distributed within the cytoplasm but not in the nuclei or other organelles. Finally we showed that 80% of MCS were labelled with FluidMAG-D with an

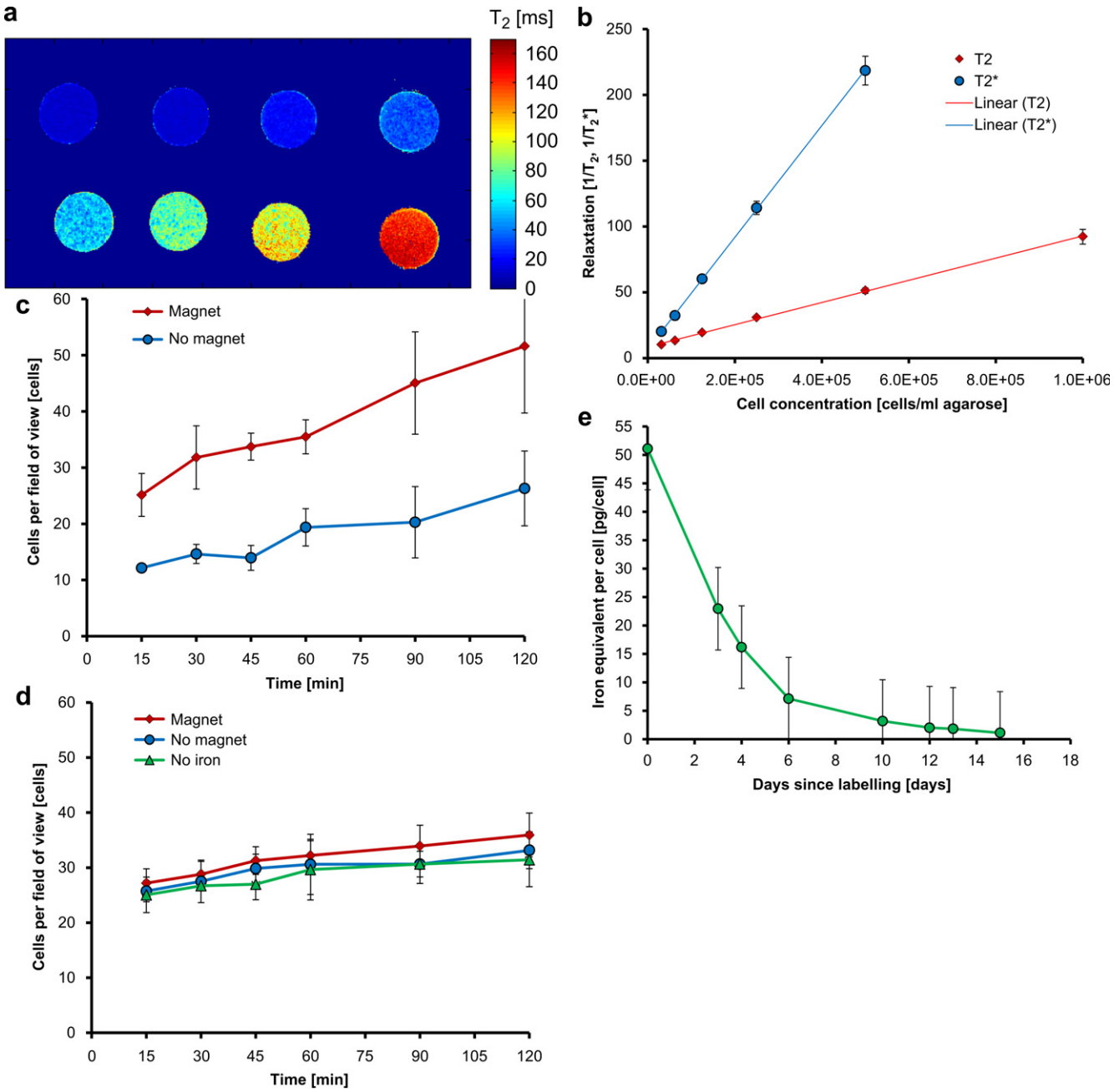

Fig. 3. Magnetic resonance T_2 contrast map (a) of tubes filled with agar containing an increasing number of magnetically labelled cells. R_2 and R_2^* relaxivities (b) of magnetically labelled MSCs. Number of magnetically labelled cells attached to a HUVEC monolayer after different time points (c) with (red line) or without (blue line) a magnetic field present. Similarly cell attachment at different time points to fibronectin coated plates (d) was assessed for unlabelled control MSCs (light green line) as well as magnetically labelled MSCs without (blue line) or with the use of a magnet (red line). Loss of iron oxide nanoparticle label (e) for FluidMAG-D labelled MSCs due to growth of the labelled cell population. (For interpretation of the references to colour in this figure legend, the reader is referred to the web version of this article.)

average internalisaiton of 57 ± 18 pg iron per cell compared to 70% and 24 ± 2 pg iron per cell for FluidMAG–P (Fig. 1c, Supplementary Fig. S5-7). We therefore selected FluidMAG-D (0.625 mg nanoparticles/ml media; ∅ 182 ± 18 nm; dextran coated; ζ-potential 1 ± 6 mV) labelling without serum starvation for further *in vitro* and *in vivo* studies.

3.2. Effect of magnetic labelling on MSC differentiation and growth factor secretion

MSCs labelled with superparamagnetic iron oxide nanoparticles showed a similar differentiation potential compared to that of unlabelled cells, except for chondrogenesis (Fig. 2a–f). There were no morphological differences between labelled and unlabelled cells. Furthermore, we did not detect any differences in secretion profiles for growth factors and cytokines (Angiopoetin-1, Activin A, IGFBP-2, CXCL4, CXCL8 and PDGF-A) between labelled and unlabelled cells (Fig. 2g,h). Labelling of MSCs with superparamagnetic iron oxide did not change the functional capacity of these cells to secret growth factors and cyotkines or their potential to differentiate and contribute to specific tissue types.

3.3. Magnetic resonance contrast properties and attachment of labelled cells

Iron oxide nanoparticles are FDA approved as magnetic resonance imaging (MRI) contrast agents for the detection of liver metastasis. The high sensitivity of these contrast agents has led to their off-label use for cell tracking in clinical trials [26,27]. We estimated the detection limit for labelled cells and the ability to monitor cell retention using MRI. Labelled cells showed strong T_2 and T_2^* contrast (R_2: $8.4 \bullet 10^{-5}$ ml cells^{-1} s^{-1}, R_2^*: $4.2 \bullet 10^{-4}$ ml cells^{-1} s^{-1}) (Fig. 3a,b) while the detection limit for cells in a single layer such as the arterial wall was approximately 200 cells/mm^3 (Supplementary Fig. S8).

We investigated the effect of magnetic forces on cell attachment to an extra cellular matrix protein (fibronectin) and endothelial cells (HUVEC monolayer), as well as magnet application time for *in vivo* experiments (Supplementary Fig. S9). Assessment of MSC attachment to endothelial cells was included in this study since some endothelial cells might still be present after arterial injury. The cell attachment rate for magnetically labelled MSC on a HUVEC monolayer was doubled compared to the control setting ($P < 0.001$, $n = 3 \times 6$) (Fig. 3c). In comparison to this, no differences were found for cell attachment rates on fibronectin coated plates for labelled cells with/without a magnetic field compared to unlabelled control cells (Fig. 3d). We selected 45 min of magnetic field application for our *in vivo* experiments, as we observed a slight decline in cell attachment rates afterwards. Finally we assessed the effect of magnetic labelling on cell growth and label dilution. Iron concentrations of labelled cells decreased rapidly following an exponential trend with a cell doubling period of roughly two days indicating unchanged growth rate and particle dilution due to cell growth (Fig. 3e).

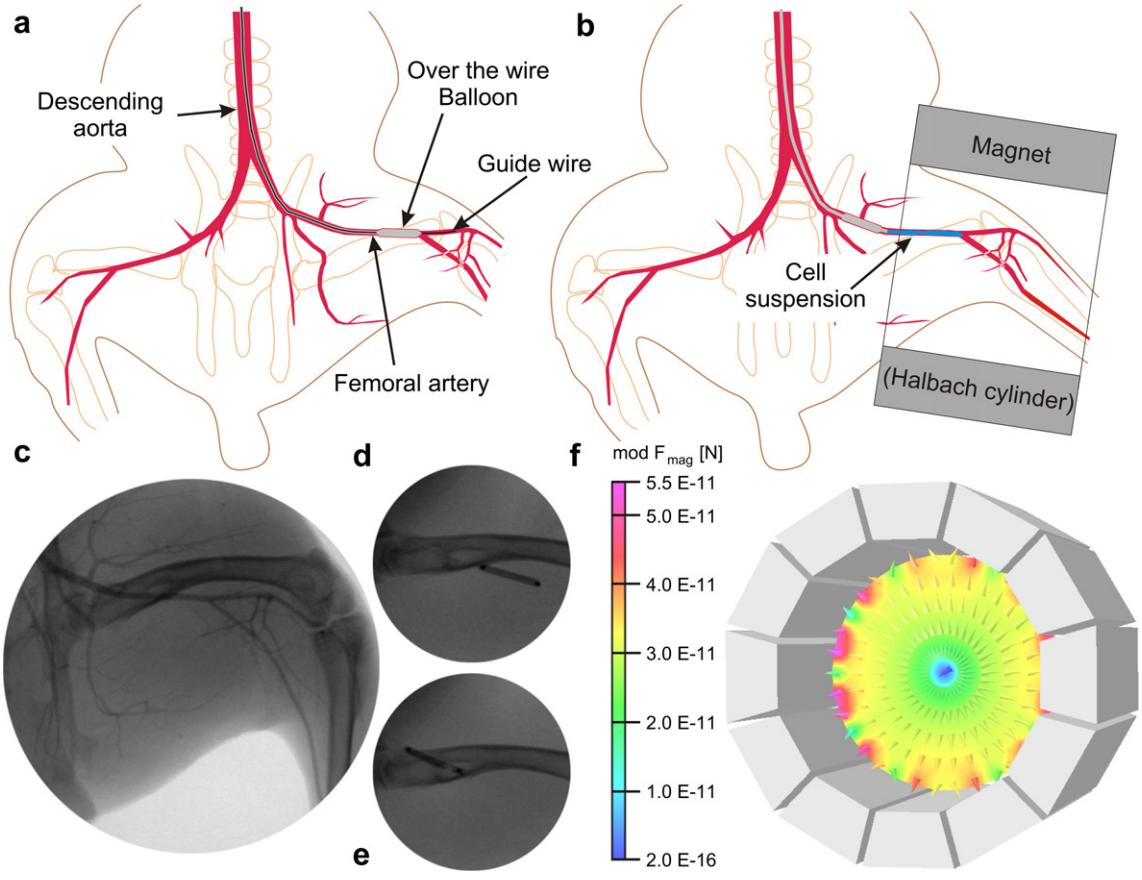

Fig. 4. Schematic of the surgical procedure for initial balloon injury to the femoral artery (a) as well as cell delivery after the blood flow has been stopped and the cylindrical magnet is put around the leg (b). Fluoroscopic images of blood vessels (c), balloon injury (d) and cell delivery (e). Simulated map for magnetic forces and cell movement (f) in the cylindrical magnet (Halbach cylinder, k3).

3.4. In vivo cell delivery procedure and cell retention 24 h after MSC delivery

For *in vivo* experiments an initial injury was caused in the femoral artery of rabbit via balloon inflation under fluoroscopic guidance (Fig. 4a, Supplementary videos V1 and V2). Following this initial injury, the balloon was retrieved 2 cm to a more proximal position and inflated to a lower pressure to stop the blood flow (Fig. 4b). A cylindrical magnet (Supplementary Fig. S10) was placed around the leg, labelled cells (100,000 allogeneic MSCs in 300 μl of saline) were delivered into the vessel lumen (Fig. 4c–f) and blood flow was restored 4 min thereafter. This external magnet was kept in place for an additional 40 min to improve cell retention and attachment. An identical control procedure was performed on the other leg, but without the use of a magnet (Supplementary Fig. S11). Cell delivery did not lead to any changes in physiological parameters or cause cardiac arrhythmias (Supplementary Fig. S12).

Supplementary video related to this article can be found at http://dx.doi.org/10.1016/j.biomaterials.2012.11.040.

High resolution MRI scans of fixed arteries 24 h post cell delivery showed magnetically labelled cells covering approximately 50% of the injured vessel circumference, while no appreciable attachment was observed for control arteries (Fig. 5d,e). The application of an external magnetic field during cell delivery lead to 6.2 fold increase in cell attachment compared to the control artery ($P < 0.05$, $n = 5$) (Fig. 5a–c, Supplementary Fig. S13). These cell densities indicate that 2% and 15% of the total amount of administered cell were retained in control and magnetic delivery arteries respectively, 24 h after delivery.

3.5. Restenosis and re-endothelialisation three weeks after MSC delivery

We found that magnetic targeting of MSCs led to a reduced femoral artery intima thickness (33 ± 15 μm) compared to control arteries (68 ± 28 μm); while media thickness was found to be very similar between groups (controls: 102 ± 13 μm; magnetic targeting: 103 ± 14 μm) (Fig. 6a,b, Supplementary Fig. S14). Accordingly a lower intima/media ratio was found for magnetic cell delivery ($P = 0.06$, $n = 5$) indicating reduced restenosis due to improved MSC retention via magnetic targeting (Fig. 6e).

The degree of re-endothelialisation was assessed via CD31 staining. No significant differences in the degree of re-endothelialisation between control and magnetic delivery arteries were observed. The luminal surfaces were almost completely covered with endothelial cells (Fig. 6c,d,f; Supplementary Fig. S15).

4. Discussion

Many regenerative medicine approaches which rely on cell delivery suffer from poor cell retention at the target site and potential unwanted side effects through global distribution [28,29]. These problems could potentially be mitigated via magnetic cell targeting. Although preclinical experiments have been performed to that end, very few have considered limitations in the scalability of this technique. However, in order to assess clinical feasibility it is necessary to design animal experiments with clinical translation in mind. While magnetic cell targeting with ferromagnetic implants such as stents have indicated clinical scalability [30,31] the same has not been demonstrated previously for magnetic cell targeting without implants [16–18]. Achieving sufficient forces for magnetic cell delivery with ferromagnetic implants is typically easier due to the high field gradients these implants generate when placed into a homogenous magnetic field. However, implants such as stents cannot be used at all locations and are problematic in long vessels which experience a lot of movement. In addition, balloon angioplasty without stent placement is the preferred first line treatment for some pathologies [3–6].

Magnetic cell targeting techniques require the labelling of cells with magnetic entities that can potentially interfere with cellular functions. Although we did not observe any effects on cytokine secretion or growth and differentiation potential except for chondrogenesis which has been reported previously [32], long term

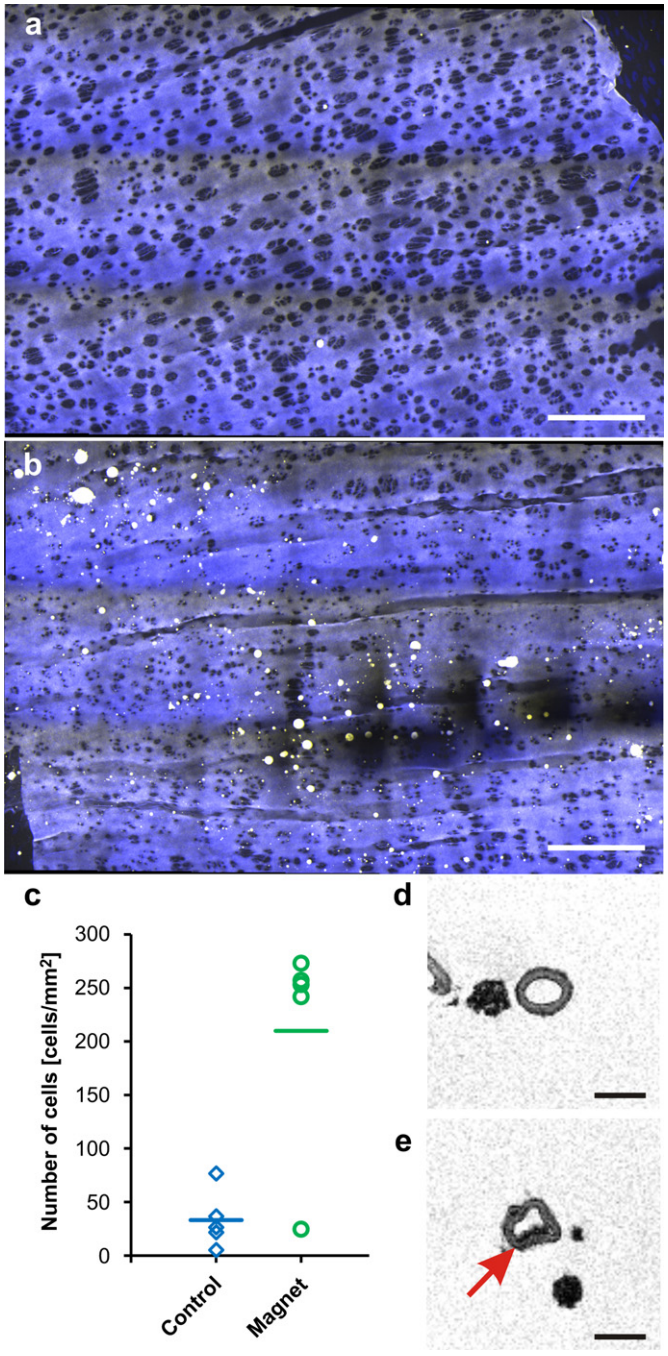

Fig. 5. Enface confocal microscopy images of magnetically and fluorescently (yellow) labelled cells 24 h after cell delivery without (a) or with a magnet (b) placed around the leg during cell delivery (scale bar: 100 μm). Scatter plot for number of cells per unit area 24 h after cell delivery (c, $n = 5$ animals for each group). Axial high resolution magnetic resonance images of artery samples 24 h after cell delivery without (d) or with (e) a magnet (scale bar: 1 mm). (For interpretation of the references to colour in this figure legend, the reader is referred to the web version of this article.)

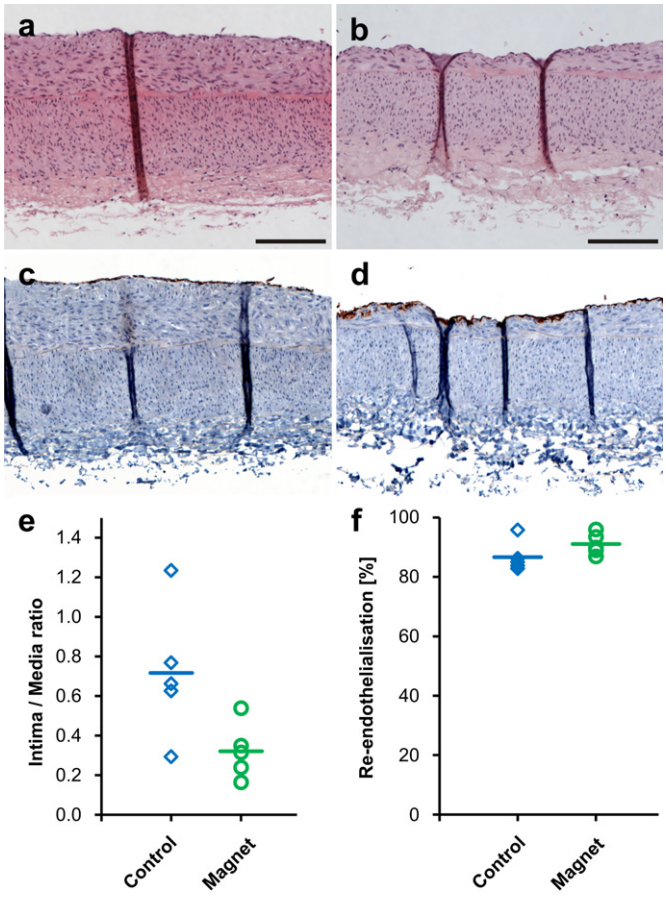

Fig. 6. Haematoxylin and eosin staining of artery sections 3 weeks after inter-arterial delivery of magnetically labelled MSCs without (a) or with a magnetic field (b) applied during cell delivery ($n = 5$ animals for each group). CD31 staining for the same artery sections without (c) or with a magnetic field (d) present during cell delivery (scale bar: 100 μm). Scatter plots for the intima/media ratio (e) and the degree of re endothelialisation (f) 3 weeks after inter-arterial cell delivery.

effects cannot be ruled out. Impaired chondrogenesis is unlikely to be a problem for our particular application, as the proposed mechanism of action is most likely via the secretion of cytokines. Previous studies have indicated that magnetic labelling can lead to elevated gene expression for up to three weeks before baseline levels are reached [33]. Even so negative long term effects have not been reported and magnetically labelled cells continue to be used for clinical trials to track cells [26,27,34]. Our cell labelling approach achieved internalisation rates which are comparable to previously reported values for MSCs [32,35,36]. Cellular uptake of nanoparticles varies between different cell lines and will require careful optimisation, in particular for cells which show lower endocytotic/pinocytotic activity such as EPCs. We selected MSCs for our study as they are easily obtainable from bone marrow and their immune suppressive properties allow allogeneic transplantation [37]. We hypothesised that local delivery of these cells might modulate the inflammatory response which is an important contributor to restenosis.

Previous mathematical simulations have indicated that cell retention in the human lower leg arteries with external magnet would only be possible close to the vessel wall where flow rates would be sufficiently low [19]. In light of that, *in vitro* cell attachment experiments were performed to estimate how long a magnet should be kept in place during *in vivo* experiments. Cell attachment rates on fibronectin coated surfaces were similar for magnetically labelled MSCs with or without the presence of a magnetic field and magnetic field gradient. This indicates that cell attachment to fibronectin, a common extra cellular matrix protein and integrin binding site, is fast and the magnetic force pulling the cells against the surface does not improve attachment. In contrast to this, the application of a magnetic field did improve the cell attachment rate on a HUVEC monolayer. Although, cell attachment to fibronectin coated surfaces and HUVEC monolayers did increase for up to 2 h, we selected a magnet application time of 45 min for practical throughput considerations.

This study demonstrates that our scalable magnetic targeting system increased cell retention after vascular injury, which reduced restenosis after three weeks, confirming data for conventional MSC delivery [23,24]. Several studies have shown that EPC delivery leads to an increased rate of re-endothelialisation and reduced restenosis [11–13]. Although we found that the endothelial layer was fully restored three weeks after initial injury, magnetic EPC delivery should be compared with magnetic MSC delivery and assessed for potential synergistic effects of combined delivery. It is possible that magnetic MSC delivery improved the rate of re-endothelialisation, but this was not possible to assess as both groups had re-endothelialised three weeks after cell delivery. Furthermore previous publications have indicated that MSCs can modulate the immune response and reduce restenosis via paracrine mechanisms [23,38]. Cellular therapies should be assessed together with their delivery techniques since localised delivery techniques such as magnetic targeting could reach therapeutic concentrations which might not be possible otherwise.

5. Conclusion

To realise the potential for magnetic control of cells in the vasculature, a new magnetic delivery strategy for targeting cellular therapies based on internalised superparamagnetic iron oxide nanoparticles has been developed. We have shown that magnetic cell delivery is feasible with a magnet design and geometry that we have also theoretically shown to be scalable for cell delivery to human leg arteries. Our magnet design achieved increased cell retention after balloon angioplasty leading to reduced restenosis in a rabbit model. This technology could be more widely adapted to different cell types and other peripheral organs, replacing inefficient systemic injection of cells, thus expanding the horizon of cardiovascular interventions.

Acknowledgements

This work was supported by the Rosetrees Trust, the Engineering and Physical Sciences Research Council (EPSRC), the British Heart Foundation (BHF) and Science Foundation Ireland (SFI), Strategic Research Cluster (SRC), Grant No. SFI: 09/SRC B1794. We would also like to thank Paul Southern (Royal Institution) for his help with SQUID measurements.

Appendix A. Supplementary data

Supplementary data related to this article can be found at http://dx.doi.org/10.1016/j.biomaterials.2012.11.040.

References

[1] Hansson GK. Inflammation, atherosclerosis, and coronary artery disease. N Engl J Med 2005;352:1685–95.
[2] Libby P, Ridker PM, Hansson GK. Progress and challenges in translating the biology of atherosclerosis. Nature 2011;473:317–25.
[3] Bosch JL, Hunink MG. Meta-analysis of the results of percutaneous transluminal angioplasty and stent placement for aortoiliac occlusive disease. Radiology 1997;204:87–96.

[4] Hirsch AT, Haskal ZJ, Hertzer NR, Bakal CW, Creager MA, Halperin JL, et al. ACC/AHA guidelines for the management of patients with peripheral arterial disease. J Vasc Interv Radiol 2006;17:1383–97.
[5] Silber S, Albertsson P, Aviles FF, Camici PG, Colombo A, Hamm C, et al. Guidelines for percutaneous coronary interventions. The task force for percutaneous coronary interventions of the European Society of Cardiology. Eur Heart J 2005;26:804–47.
[6] Vroegindeweij D, Vos LD, Tielbeek AV, Buth J, vd Bosch HC. Balloon angioplasty combined with primary stenting versus balloon angioplasty alone in femoropopliteal obstructions: a comparative randomized study. Cardiovasc Intervent Radiol 1997;20:420–5.
[7] Landau C, Lange RA, Hillis LD. Percutaneous transluminal coronary angioplasty. N Engl J Med 1994;330:981–93.
[8] Libby P, Schwartz D, Brogi E, Tanaka H, Clinton SK. A cascade model for restenosis. A special case of atherosclerosis progression. Circulation 1992;86: III47–52.
[9] Monraats PS, Agema W RP, Jukema JW. Genetic predictive factors in restenosis. Pathol Biol 2004;52:186–95.
[10] Bangalore S, Kumar S, Fusaro M, Amoroso N, Kirtane AJ, Byrne RA, et al. Outcomes with various drug eluting and bare metal stents in patients with diabetes mellitus: mixed treatment comparison analysis fo 22,844 patient years of follow-up from randomised trials. BMJ 2012;345:e5170.
[11] Gulati R, Jevremovic D, Peterson TE, Witt TA, Kleppe LS, Mueske CS, et al. Autologous culture-modified mononuclear cells confer vascular protection after arterial injury. Circulation 2003;108:1520–6.
[12] He T, Smith LA, Harrington S, Nath KA, Caplice NM, Katusic ZS. Transplantation of circulating endothelial progenitor cells restores endothelial function of denuded rabbit carotid arteries. Stroke 2004;35:2378–84.
[13] Kong D, Melo LG, Mangi AA, Zhang L, Lopez-llasaca M, Perrella MA, et al. Enhanced inhibition of neointimal hyperplasia by genetically engineered endothelial progenitor cells. Circulation 2004;109:1769–75.
[14] Pankhurst QA, Connolly J, Jones SK, Dobson J. Applications of magnetic nanoparticles in biomedicine. J Phys D: Appl Phys 2003;36:R167.
[15] Dames P, Gleich B, Flemmer A, Hajek K, Seidl N, Wiekhorst F, et al. Targeted delivery of magnetic aerosol droplets to the lung. Nat Nanotechnol 2007;2: 495–9.
[16] Hofmann A, Wenzel D, Becher UM, Freitag DF, Klein AM, Eberbeck D, et al. Combined targeting of lentiviral vectors and positioning of transduced cells by magnetic nanoparticles. Proc Natl Acad Sci U S A 2009;106:44–9.
[17] Kyrtatos PG, Lehtolainen P, Junemann-Ramirez M, Garcia-Prieto A, Price AN, Martin JF, et al. Magnetic tagging increases delivery of circulating progenitors in vascular injury. JACC Cardiovasc Interv 2009;2:794–802.
[18] Cheng K, Li TS, Malliaras K, Davis DR, Zhang Y, Marban E. Magnetic targeting enhances engraftment and functional benefit of iron-labeled cardiosphere-derived cells in myocardial infarction. Circ Res 2010;106:1570–81.
[19] Riegler J, Lau KD, Garcia-Prieto A, Price AN, Richards T, Pankhurst QA, et al. Magnetic cell delivery for peripheral arterial disease: a theoretical framework. Med Phys 2011;38:3932–43.
[20] Fernandez-Aviles F, San Roman JA, Garcia-Frade J, Fernandez ME, Penarrubia MJ, de la Fuente L, et al. Experimental and clinical regenerative capability of human bone marrow cells after myocardial infarction. Circ Res 2004;95:742–8.
[21] Tanaka K, Sata M, Hirata Y, Nagai R. Diverse contribution of bone marrow cells to neointimal hyperplasia after mechanical vascular injuries. Circ Res 2003; 93:783–90.
[22] Werner N, Junk S, Laufs U, Link A, Walenta K, Bohm M, et al. Intravenous transfusion of endothelial progenitor cells reduces neointima formation after vascular injury. Circ Res 2003;93:e17–24.
[23] Forte A, Finicelli M, Mattia M, Berrino L, Rossi F, De Feo M, et al. Mesenchymal stem cells effectively reduce surgically induced stenosis in rat carotids. J Cell Physiol 2008;217:789–99.
[24] Wang CH, Cherng WJ, Yang NI, Kuo LT, Hsu CM, Yeh HI, et al. Late-outgrowth endothelial cells attenuate intimal hyperplasia contributed by mesenchymal stem cells after vascular injury. Arterioscler Thromb Vasc Biol 2008;28:54–60.
[25] Sharif F, Hynes SO, Cooney R, Howard L, McMahon J, Daly K, et al. Gene-eluting stents: adenovirus-mediated delivery of eNOS to the blood vessel wall accelerates re-endothelialization and inhibits restenosis. Mol Ther 2008;16: 1674–80.
[26] de Vries IJ, Lesterhuis WJ, Barentsz JO, Verdijk P, van Krieken JH, Boerman OC, et al. Magnetic resonance tracking of dendritic cells in melanoma patients for monitoring of cellular therapy. Nat Biotechnol 2005;23:1407–13.
[27] Zhu J, Zhou L, XingWu F. Tracking neural stem cells in patients with brain trauma. N Engl J Med 2006;355:2376–8.
[28] Freyman T, Polin G, Osman H, Crary J, Lu M, Cheng L, et al. A quantitative, randomized study evaluating three methods of mesenchymal stem cell delivery following myocardial infarction. Eur Heart J 2006;27:1114–22.
[29] Hou D, Youssef EA, Brinton TJ, Zhang P, Rogers P, Price ET, et al. Radiolabeled cell distribution after intramyocardial, intracoronary, and interstitial retrograde coronary venous delivery: implications for current clinical trials. Circulation 2005;112:I150–6.
[30] Pislaru SV, Harbuzariu A, Gulati R, Witt T, Sandhu NP, Simari RD, et al. Magnetically targeted endothelial cell localization in stented vessels. J Am Coll Cardiol 2006;48:1839–45.
[31] Polyak B, Fishbein I, Chorny M, Alferiev I, Williams D, Yellen B, et al. High field gradient targeting of magnetic nanoparticle-loaded endothelial cells to the surfaces of steel stents. Proc Natl Acad Sci U S A 2008;105:698–703.
[32] Arbab AS, Yocum GT, Kalish H, Jordan EK, Anderson SA, Khakoo AY, et al. Efficient magnetic cell labeling with protamine sulfate complexed to ferumoxides for cellular MRI. Blood 2004;104:1217–23.
[33] Kedziorek DA, Muja N, Walczak P, Ruiz-Cabello J, Gilad AA, Jie CC, et al. Gene expression profiling reveals early cellular responses to intracellular magnetic labeling with superparamagnetic iron oxide nanoparticles. Magn Reson Med 2010;63:1031–43.
[34] Toso C, Vallee JP, Morel P, Ris F, Demuylder-Mischler S, Lepetit-Coiffe M, et al. Clinical magnetic resonance imaging of pancreatic islet grafts after iron nanoparticle labeling. Am J Transplant 2008;8:701–6.
[35] Frank JA, Miller BR, Arbab AS, Zywicke HA, Jordan EK, Lewis BK, et al. Clinically applicable labeling of mammalian and stem cells by combining superparamagnetic iron oxides and transfection agents. Radiology 2003;228:480–7.
[36] Loebinger MR, Kyrtatos PG, Turmaine M, Price AN, Pankhurst Q, Lythgoe MF, et al. Magnetic resonance imaging of mesenchymal stem cells homing to pulmonary metastases using biocompatible magnetic nanoparticles. Cancer Res 2009;69:8862–7.
[37] Di Nicola M, Carlo-Stella C, Magni M, Milanesi M, Longoni PD, Matteucci P, et al. Human bone marrow stromal cells suppress T-lymphocyte proliferation induced by cellular or nonspecific mitogenic stimuli. Blood 2002;99:3838–43.
[38] Pati S, Gerber MH, Menge TD, Wataha KA, Zhao Y, Baumgartner JA, et al. Bone marrow derived mesenchymal stem cells inhibit inflammation and preserve vascular endothelial integrity in the lungs after hemorrhagic shock. PLos One 2011;6:e25171.